

# EXPERIMENTAL AND COMPUTATIONAL STUDY OF THE THERMAL DECOMPOSITION OF URONIUM NITRATE (UREA NITRATE)

Reiko I. Hiyoshi  
National Research Institute of Police Science  
Chiba 277-0882, Japan

Thomas B. Brill  
University of Delaware  
Newark, DE 19716

Yuji Kohno, Osamu Takahashi and Ko Saito  
Hiroshima University  
Hiroshima 739-8526, Japan

The thermal decomposition process of uronium nitrate (urea nitrate) explosive was determined at various conditions by T-jump/FT-IR spectroscopy. The behavior of the decomposition products suggests that there are two main decomposition pathways, which depend on the pressure and temperature. The thermochemistry of the two channels was evaluated qualitatively. Plausible transition states and selected infrared frequencies were calculated by *Ab initio* quantum mechanical methods. According to *Ab initio* MO calculations, transition states exits for the first stage of the proposed reaction scheme.

## INTRODUCTION

Uronium nitrate (or urea nitrate, UN, which is formed by the reaction of urea with nitric acid) is serviceable as a component of fertilizer<sup>1,2</sup> and as an explosive.<sup>3</sup> It was used in the first terrorist attack on the World Trade Center in New York City in 1993. UN explodes, but is not in practical use because of its strong acidity. The explosive properties of UN, such as the sensitivities and detonation velocity, have been determined recently by Hiyoshi and Nakamura.<sup>4,5</sup> The friction sensitivity and impact sensitivity were low. The shock sensitivity was measured by the

card-gap test, and the critical shock initiation pressure was found to be 2.2-2.6 GPa. The detonation velocity of UN reached 5300m/s, which is comparable to that of emulsion explosives, and depended on the bulk density. UN is a type II explosive in the categorization of Price.<sup>6</sup>

This paper describes the thermal decomposition process of UN following heating to specific temperatures at 2000°C/s using T-jump/FT-IR spectroscopy. The decomposition pathways were determined, and *Ab initio* MO calculations were used to study the structures and energetics of reactants,

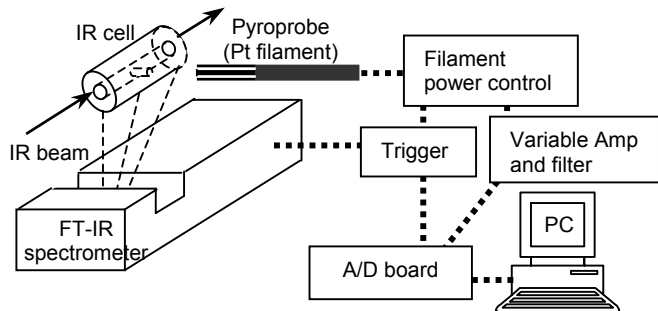


**FIGURE 1. T-JUMP/FT-IR SYSTEM**

products, intermediates and transition states for the probable reaction mechanism.

## EXPERIMENTAL

The T-jump/FT-IR system is diagrammed in Fig. 1. The details were described previously.<sup>7</sup> In this technique the sample was placed as a thin film on a polished Pt filament inside the closed cell. The control circuit enabled the filament to be heated at rates up to 20000°C/s to a chosen temperature and held there for 20s. The heating rate was 2000°C/s in this study, and thermal behavior of the sample was determined by recording the control voltage trace of the Pt filament. Simultaneously, 4 Hz IR spectra were recorded of the products leaving the surface. These experiments were performed in both Ar and a simulated air atmosphere (80% N<sub>2</sub> – 20% O<sub>2</sub>) at pressures of 1-21 atm. UN wetted with 25% water was obtained from Tokyo Kasei Kogyo Co., Ltd. It was dried with flowing air for three hours, and stored in a desiccator.

The concentrations of the gaseous products were determined by first-order spectral resolution with least-squares optimization using quadratic programming constraints.<sup>8</sup> The spectra were processed as matrices and calibration matrices for known products were subtracted from the raw data. The concentrations of all species were obtained by minimizing the residual. Calibration spectra

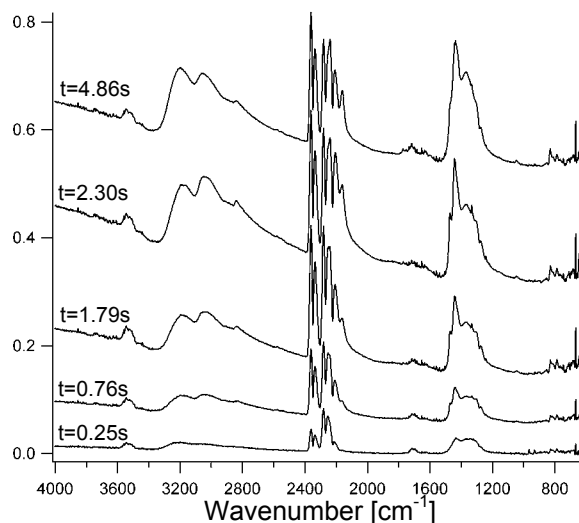


**FIGURE 2. TIME DEPENDENCE OF THE IR SPECTRA OF DECOMPOSITION PRODUCTS OF UN IN AR (8 ATM, 400°C)**

for ammonium nitrate (AN) and the unknown products were not available, so their concentrations were calculated with arbitrarily chosen fitting constants so that the trends could be observed.

*Ab initio* MO calculations were carried out with the GAUSSIAN-98<sup>9</sup> program package. The basis sets implemented in the program were employed without modification. The geometries of reactants, products, intermediates, and TSs were fully optimized without symmetry constraints by the energy gradient methods. All optimized geometries were obtained by using the 6-31++G(2d,p) (split-valence plus diffuse functions plus 2dp-polarization functions) basis set. Vibrational frequencies were calculated by using the analytical second derivatives at the 6-31++G(2d,p) level to confirm the stationary structures and correct for the zero-point vibrational energy.

Intrinsic reaction coordinate (IRC) calculations using internal coordinates were performed to verify that computed transition

states were saddle points between reactants and products.

## RESULTS AND DISCUSSION

The pyrolysis data discussed in this paper were obtained in an Ar atmosphere. However, experiments were also conducted in a simulated air atmosphere. The results are the same, except for  $\text{NO}_2$ , indicating that UN decomposes in the condensed phase without participation of the surrounding atmosphere. This finding is consistent with recent work, which reveals that the surrounding atmosphere only affects compounds having a non-negligible vapor pressure.<sup>10</sup> The concentration of  $\text{NO}_2$  in air increases with time due to oxidation of  $\text{NO}$  by  $\text{O}_2$ , whereas little  $\text{NO}_2$  is formed when Ar is the surrounding atmosphere.

Figure 2 shows a time series of IR spectra of the gaseous products from UN heated at  $400^\circ\text{C}$  in 8 atm of Ar. The initial gaseous species are primarily  $\text{HNCO}$  ( $2281\text{cm}^{-1}$ ,  $2256\text{cm}^{-1}$ ),  $\text{CO}_2$  ( $2359\text{cm}^{-1}$ ,  $2341\text{cm}^{-1}$ ),  $\text{N}_2\text{O}$  ( $2235\text{cm}^{-1}$ ,  $2214\text{cm}^{-1}$ ),  $\text{NH}_3$  ( $966\text{cm}^{-1}$ ,  $930\text{cm}^{-1}$ ), and  $\text{H}_2\text{O}$  (rotational structure centered at about  $1600\text{cm}^{-1}$ ). AN and an unidentified product dominate at longer times. These data were quantified by multivariate regression and plotted in Fig. 3 for conditions of  $300^\circ\text{C}$  and  $500^\circ\text{C}$  in 8 atm and 21 atm. Fig. 4 repeats Fig. 3 except that the AN and an unknown are removed for clarity. More  $\text{CO}_2$  and  $\text{N}_2\text{O}$  relative to  $\text{HNCO}$  (*vide infra*) are produced at the harsher conditions. The concentration of  $\text{NO}$  (from  $\text{HNO}_3$  decomposition) is low, but has a tendency to be produced at the higher temperatures and pressures.

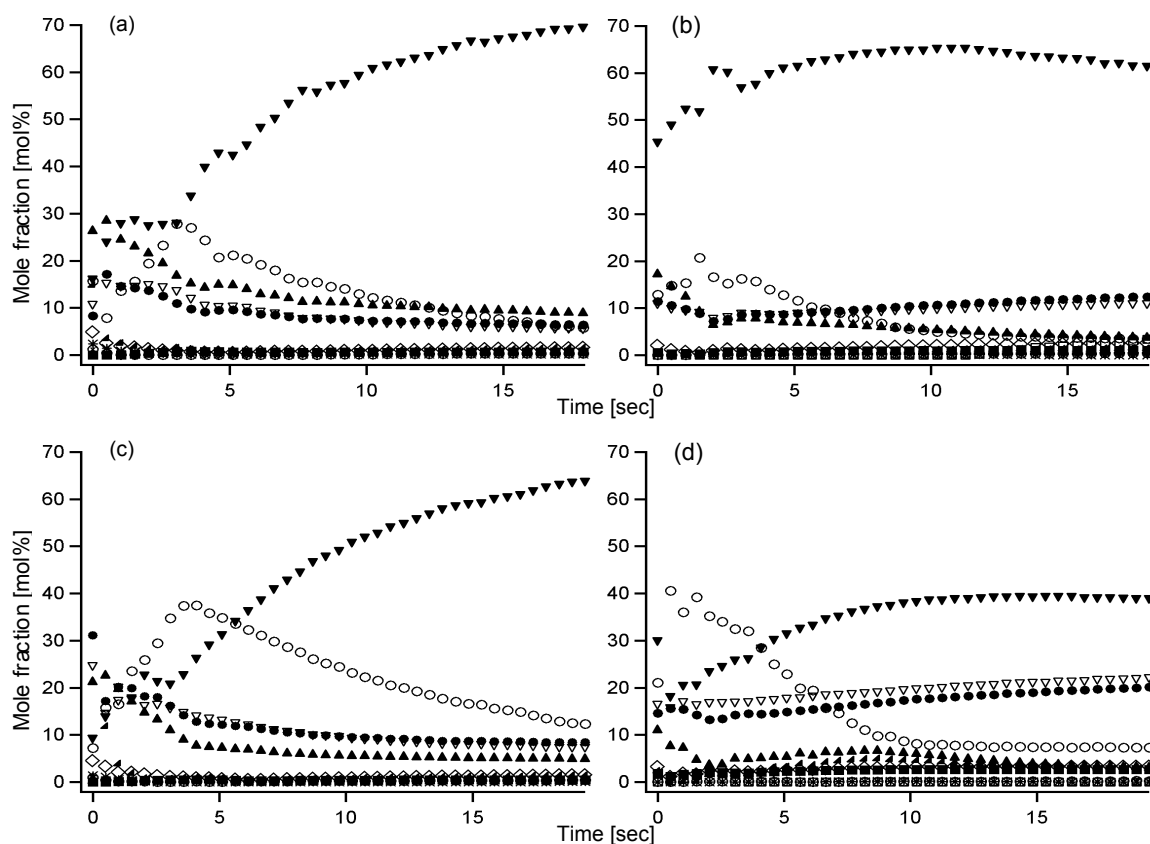


**FIGURE 3. DECOMPOSITION PRODUCTS OF UN IN AR**  
**(A)8ATM, 300°C, (B)8ATM, 500°C, (C)21ATM,300°C, (D)21ATM,500°C**  
 ●:CO<sub>2</sub>, ■:NO<sub>2</sub>, ▽:N<sub>2</sub>O, ▲:HNCO, ◇:H<sub>2</sub>O, ◻:NH<sub>3</sub>, ◻:NO, ▼:AN, ○:Unknown

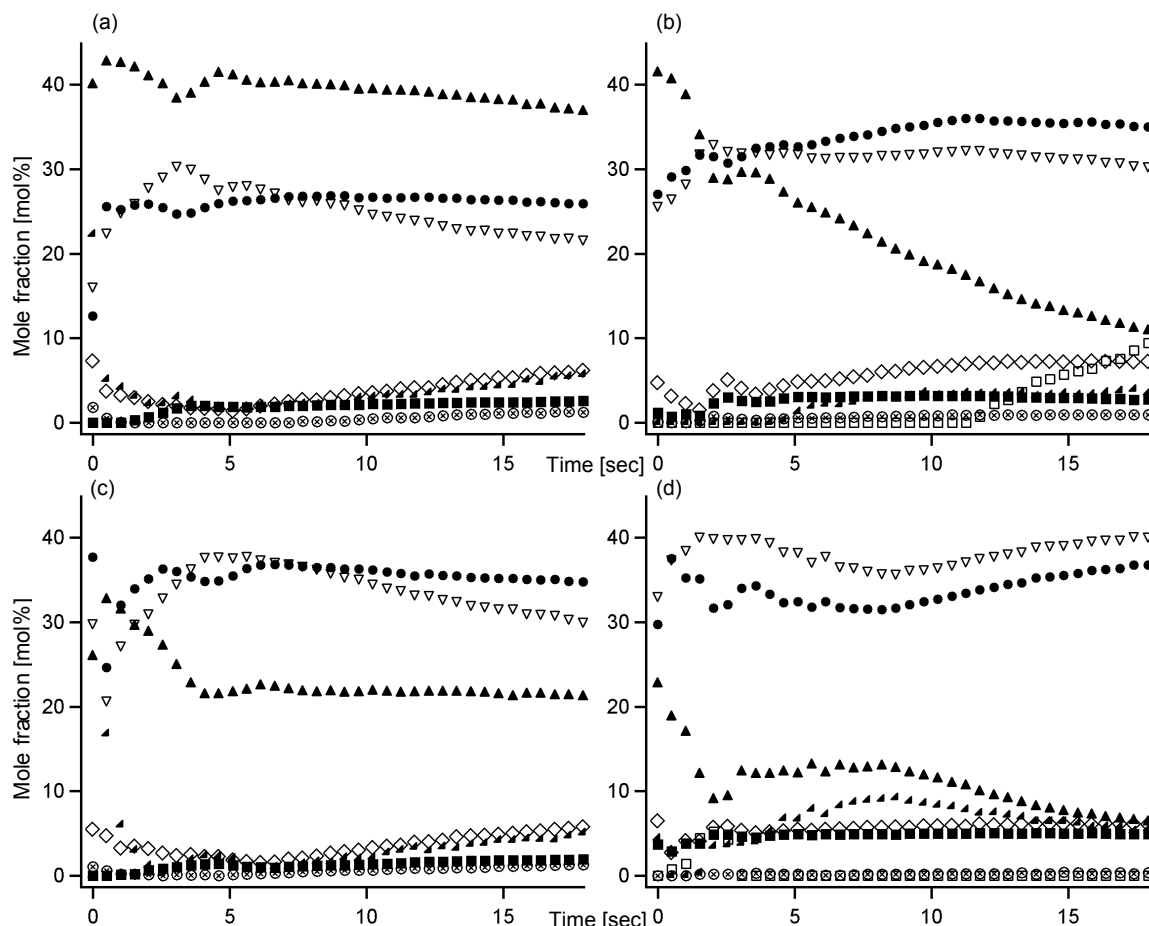
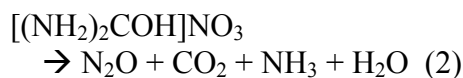
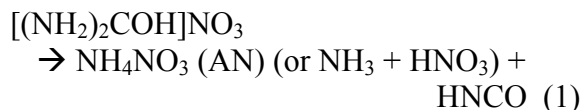


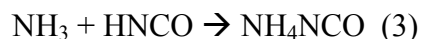
**FIGURE 4. DECOMPOSITION PRODUCTS OF UN IN AR (WITHOUT AN AND UNKNOWN SPECIES)**  
**(A)8ATM, 300°C, (B)8ATM, 500°C, (C)21ATM,300°C, (D)21ATM,500°C**  
 ● :CO<sub>2</sub>, ■ :NO<sub>2</sub>, ▽ :N<sub>2</sub>O, ▲ :HNCO, ◇ :H<sub>2</sub>O, ▲ :NH<sub>3</sub>, □ :NO

A typical residual spectrum from subtraction of the known products from UN decomposition is shown in Fig. 5 which helps identify the remaining products. The band at 1430cm<sup>-1</sup>, and the broad Fermi resonance triplet at 2950-3220cm<sup>-1</sup> were assigned to AN. The multiple bands at 2150-2300cm<sup>-1</sup> and 1200-1500cm<sup>-1</sup> are assumed to be from NH<sub>4</sub>NCO, NH<sub>4</sub>OCN, and species containing –C=N and –C≡N, such as cyanamide, dicyandiamide, and related cyclic azines.<sup>11</sup> Additionally, the *Ab initio* MO calculations for vibrational frequencies confirm that the strong band at 2160cm<sup>-1</sup> corresponds to the NCO symmetric stretching vibration.

Based on these experiments, there appear to be two principal reaction channels in the decomposition of UN:



The NH<sub>3</sub> from path (2) and the HNCO from path (1) partially combine to produce NH<sub>4</sub>NCO in the gaseous phase (reaction 3). Some of the NH<sub>4</sub>OCN isomer is also possible.



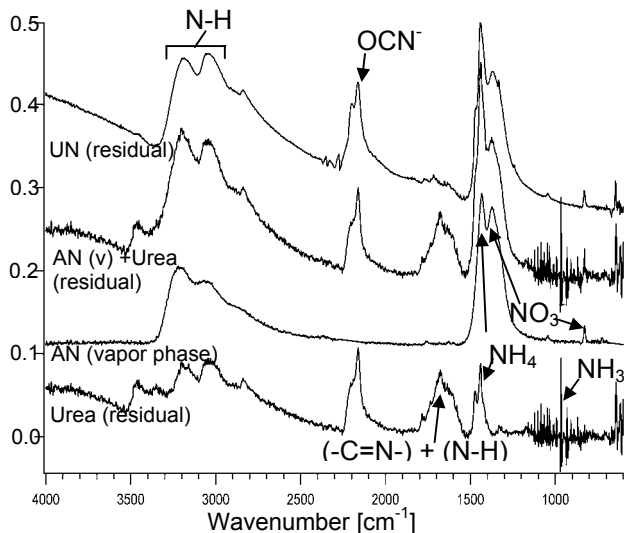


**FIGURE 5. IR SPECTRA OF DECOMPOSITION PRODUCTS OF UN AND UREA IN AR (PRESSURE: 8ATM, PYROPROBE:400°C)**

HNO<sub>3</sub> is not evident in Fig. 2, but it appears at the beginning of the decomposition reaction in IR spectra below 400°C, and exists for 3-5 seconds. Therefore, at the early stage of the reaction some of the UN decomposes to HNO<sub>3</sub> and urea. The decomposition products

of urea at the T-jump conditions are NH<sub>4</sub>NCO (reaction 4) and at least one unknown product. This rearrangement is fast enough that the IR bands of gaseous urea are never seen in the spectra.



Support for the conclusions above is based on the concentrations of the species and assignments of the AN and NH<sub>4</sub>NCO species in the spectra of the gaseous phase. *Ab initio* MO calculations were undertaken to determine the assignments of unknown frequencies and transition states for the thermal decomposition channels. Two transition state structures were determined. Fig.6(a), (b) and (c) show geometries of transition states and intermediate products for the decomposition reaction paths of UN optimized at 6-31++G(2d,p) level. Fig.6(a) shows an optimized geometry of a transition state (TS(1)) initiating an internal proton transfer reaction. Arrows indicate the displacement vectors of normal mode with an

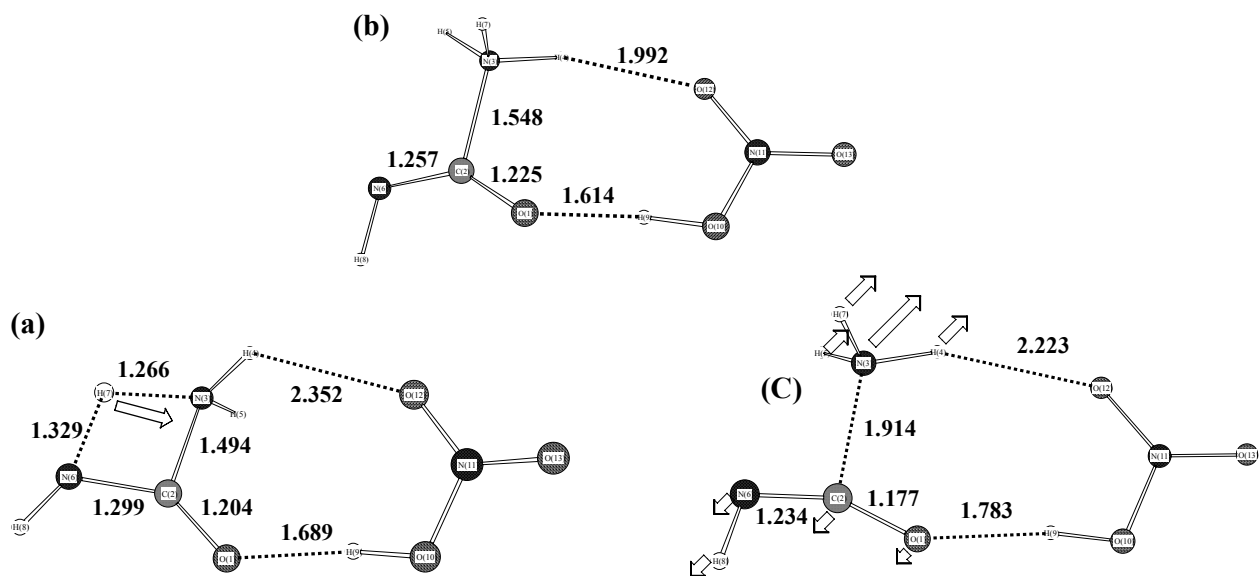


**FIGURE 6. (A)HF/6-31++G(2D,P) OPTIMIZED GEOMETRIES AND DISPLACEMENT VECTORS OF NORMAL MODE WITH AN IMAGINARY FREQUENCY(2162.9I CM-1) FOR THE TRANSITION STATE(TS1). BOND DISTANCES ARE IN ANGSTROMS. (B)HF/6-31++G(2D,P) OPTIMIZED GEOMETRY OF INTERMEDIATE(1). BOND DISTANCES ARE IN ANGSTROMS. (C) HF/6-31++G(2D,P) OPTIMIZED GEOMETRIES AND DISPLACEMENT VECTORS OF NORMAL MODE WITH AN IMAGINARY FREQUENCY(401.1I CM-1) FOR THE TRANSITION STATE(TS2). BOND DISTANCES ARE IN ANGSTROMS.**

imaginary frequency. The vibrational frequency ( $2162.9i\text{ cm}^{-1}$ ) corresponds to the H---N(3) stretching mode leading to an internal proton transfer reaction. After TS(1), an intermediate (INT(1), Fig.6(b)) is formed by internal proton transfer. By IRC calculations, the changes (TS(1)  $\rightarrow$  INT(1)) have been confirmed. These IRC calculations show that transition state TS(1) is a saddle point connecting the reactant and products. This process, UN  $\rightarrow$  TS(1) has an activation energy of 64.2kcal/mol. These calculated results seem to support the experimental results which observed at the early stage of UN decomposition. INT(1) proceeds to TS(2) ( $401i\text{ cm}^{-1}$ , Fig.6(c)). The directions of the displacement vectors of TS(2) strongly indicate the occurrence of the decomposition to produce  $\text{NH}_3$ , HNCO and  $\text{HNO}_3$ . The activation energy for this reaction is 1.9kcal/mol. Therefore, after TS(2),  $\text{NH}_3$ , HNCO and  $\text{HNO}_3$  should be rapidly generated. These results suggest strongly that this decomposition occurs via internal hydrogen transfer from the one of the amino group to the other  $-\text{NH}_2$  to produce  $\text{NH}_3$ . Subsequently, HNCO forms accompanied by ( $\text{NH}_3 + \text{HNO}_3$ ) or AN. Thus, the route to reaction (1) is clearly defined quantum mechanically. Reaction (2) is too global to be characterizable in this manner.

The thermochemistry of (1) and (2) can be qualitatively evaluated experimentally from the gaseous products and the thermal traces. HNCO and  $\text{CO}_2$  are unique products of the two channels. The heat of reaction of (1) is +29 kcal/mol while that of (2) is -8.8 kcal/mol. The low amount of heat released by these reactions of UN is primarily the result of the very negative heat of formation of UN (-134 kcal/mol). Hence during pyrolysis, the process only becomes exothermic overall when the (2) strongly dominates. The fact that the HNCO concentration is high at the beginning suggests that the endothermic reaction (1) dominates initially. The control

voltage trace (Fig.7) indeed shows endothermicity (positive control voltage deflection) at the onset of the decomposition. This endothermic response is not the result of melting. This may imply proton transfer. As the reaction progresses, the  $\text{CO}_2$  and  $\text{N}_2\text{O}$  concentrations rise as a result of the exothermic channel and the thermal trace indeed shows mild exothermicity (negative deflection of the control voltage). Consistent with the thermochemical estimate, Figure 7 shows that the overall exothermicity of UN is much less than that of nitroglycerin (NG).

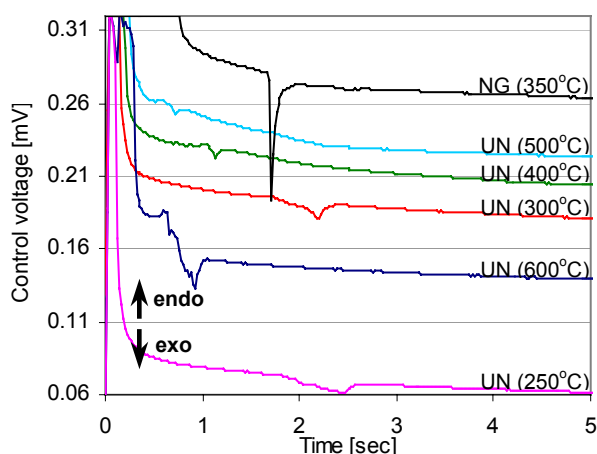


**FIGURE 7. CONTROL VOLTAGE TRACES OF UN AND NG (8ATM IN AR)**

The early stage HNCO/ $\text{CO}_2$  concentration ratio exhibits little temperature dependence below  $500^\circ\text{C}$  (Fig. 8). There is only a faster evolution rate of the species at higher temperature. The data at  $600^\circ\text{C}$  show that  $\text{CO}_2$  is beginning to dominate the other products and that  $\text{H}_2\text{O}$  has higher concentration (Fig. 9). Hence, UN is beginning to shift toward the detonation-like products  $\text{CO}_2$  and  $2\text{H}_2\text{O}$ . IR inactive products ( $3/2\text{N}_2$  and  $1/2\text{H}_2$ ) also must be present at  $600^\circ\text{C}$  to balance the stoichiometry. The decomposition process becomes correspondingly more exothermic as  $\text{CO}_2$  and  $\text{H}_2\text{O}$  become more dominant products.

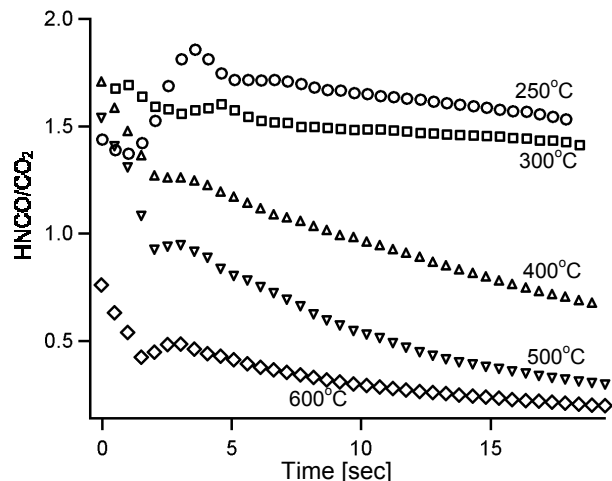


FIGURE 8. HNCO/CO<sub>2</sub> RATIO IN AR (8ATM)

## CONCLUSIONS

The evidence to date is that UN decomposes primarily in the condensed phase by two global, temperature-dependent reaction channels. The lower temperature channel is endothermic, while the higher temperature channel is exothermic. As the pyrolysis temperature is increased further, the gaseous products appear more detonation-like. In our present calculation, there are four important products (NH<sub>3</sub>, HNO<sub>3</sub>, HNCO and NH<sub>4</sub>NCO) through the reaction paths. The route to initial endothermic channel (1) is clearly defined quantum mechanically. Thus, both flash pyrolysis data and quantum mechanical calculations are mutually consistent.

## ACKNOWLEDGMENTS

RIH thanks the Ministry of Education, Sports, Science and Technology of Japan for the financial support. RIH is also grateful to Mr. J. Nakamura and Dr. H. Arisawa for their suggestions and advice. TBB gratefully acknowledges to SERDP for support on CP1193. YK, OT and KS are grateful to a Grant-in-Aid on research for the future

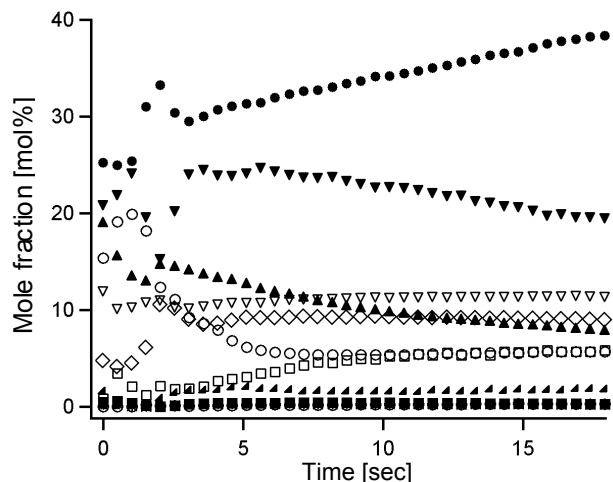


FIGURE 9. DECOMPOSITION PRODUCTS OF UN IN AR (PRESSURE:8ATM, PYROPROBE:600°C)

●:CO<sub>2</sub>, ■:NO<sub>2</sub>, ▽:N<sub>2</sub>O, ▲:HNCO, ◇:H<sub>2</sub>O,  
▲:NH<sub>3</sub>, □:NO, ▽:AN, ○:Unknown

“Photoscience” (JSPS-RFTF-98P01202) from Japan Society for the Promotion of science.

## REFERENCES

1. T. R. Narayanan Kutty and A. R. Vasudeva Murthy, “Physico-chemical Properties of Urea Nitrate: Part I – Preparation and Characterization”, *Ind. J. Tech.*, vol. 10, pp. 305-308, 1972.
2. H. Roy and H. Acharyya, “Thermal Studies on Some Urea Complexes of Compound Fertilizers”, *Technology*, vol. 7(4), pp. 281-285, 1970.
3. K. Hino and J. Sato, “Industrial Explosives Containing Urea Derivatives (N-Explosives) Part I”, *Kogyo Kagaku Kyokaiishi*, vol. 12(2), pp. 106-108, 1952.
4. R. I. Hiyoshi and J. Nakamura, “Explosion Properties of Urea Nitrate and its Analysis”, *Proc. 6<sup>th</sup> Int. Symp. Anal. Det. Expl.* Prague, CZ, 1998, paper15.
5. R. I. Hiyoshi and J. Nakamura, “Explosion Properties of Urea Nitrate”, *Kagaku Gakkaishi*, vol. 61(3), pp.120-123, 2000.

6. D. Price, "Contrasting Patterns in the Behavior of High Explosives", *Eleventh Symp. (Int) Combustion*, The Combustion Institute, Pittsburgh, PA, pp. 693-702, 1967.
7. T. B. Brill, P. J. Brush, K. J. James, J. E. Shepherd and K. J. Pfeiffer, "T-Jump/FT-IR Spectroscopy: A New Entry into the Rapid Isothermal Pyrolysis Chemistry of Solids and Liquids," *Appl. Spectrosc.*, vol. 46(6), pp. 900-911, 1992.
8. H. Arisawa and T. B. Brill, "Kinetics and Mechanisms of Flash Photolysis of Poly(methyl methacrylate) (PMMA)", *Combust. Flame*, vol. 106, pp. 415-426, 1997.
8. H. Arisawa, "Kinetics of Pathways of Polymer Binder/fuel Pyrolysis under combustion-like Conditions", Ph.D. Thesis University of Delaware, 1997.
9. M. J. Frisch, G. W. Trucks, H. B. Schlegel, G. E. Scuseria, M. A. Robb, J. R. Cheeseman, V. G. Zakrzewski, J. A. Montgomery, R. E. Stratmann, Jr., J. C. Burant, S. Dapprich, J. M. Millam, A. D. Daniels, K. N. Kudin, M. C. Strain, O. Farkas, J. Tomasi, V. Barone, M. Cossi, R. Cammi, B. Mennucci, C. Pomelli, C. Adamo, S. Clifford, J. Ochterski, G. A. Petersson, P. Y. Ayala, Q. Cui, K. Morokuma, D. K. Malick, A. D. Rabuck, K. Raghavachari, J. B. Foresman, J. Cioslowski, J. V. Ortiz, B. B. Stefanov, G. Liu, A. Liashenko, P. Piskorz, I. Komaromi, R. Gomperts, R. L. Martin, D. J. Fox, T. Keith, M. A. Al-Laham, C. Y. Peng, A. Nanayakkara, C. Gonzalez, M. Challacombe, P. M. W. Gill, B. Johnson, W. Chen, M. W. Wang, J. L. Andres, C. Gonzalez, M. Head-Gordon, E. S. Replogle, J. A. Pople, GAUSSIAN98, Revision A.4, Gaussian Inc., Pittsburgh, PA, 1998.
10. R. I. Hiyoshi and T. B. Brill, "Thermal Decomposition of Energetic Materials 83. Comparison of the Pyrolysis of Energetic Materials in Air vs. Argon," *Prop. Explos. Pyrotech.* in press.
11. C. E. Stoner, Jr. and T. B. Brill, "Thermal Decomposition of Energetic Materials 46. The Formation of Melamine-like Cyclic Azines as a Mechanism for Ballistic Modification of Composite Propellants by DCD, DAG and DAF," *Combust. Flame*, vol. 83, pp. 302-308, 1991.